Kinesthetic illusion of wrist movement activates motor-related areas

Eiichi Naito[1,2,CA] and H. Henrik Ehrsson[1,3]

[1]Division of Human Brain Research, Department of Neuroscience, Karolinska Institute, Retzius Väg 8 A3:3 S-171 77 Stockholm, Sweden; [2]Faculty of Human Studies, Kyoto University, Sakyo-ku, Kyoto, 606-8501, Japan; [3]Motor Control Laboratory, Department of Woman and Child Health, Karolinska Institute, Stockholm, Sweden

[CA]Corresponding Author

Received 22 August 2001; accepted 14 September 2001

We used positron emission tomography (PET) to test the hypothesis that illusory movement of the right wrist activates the motor-related areas that are activated by real wrist movements. We vibrated the tendons of the relaxed right wrist extensor muscles which elicits a vivid illusory palmar flexion. In a control condition, we vibrated the skin surface over the processes styloideus ulnae, which does not elicit the illusion, using the identical frequency (83 Hz). We provide evidence that kinesthetic illusory wrist movement activates the contralateral primary sensorimotor cortices, supplementary motor area (SMA) and cingulate motor area (CMA). These areas are also active when executing the limb movement. *NeuroReport* 12:3805–3809 © 2001 Lippincott Williams & Wilkins.

Key words: Cingulate motor area (CMA); Illusory wrist movements; Limb position; Primary sensorimotor cortices (SM1); Supplementary motor area (SMA)

INTRODUCTION

Vibration stimuli of ~80 Hz applied to the tendons of muscles can elicit illusory movements by stimulating the muscle spindle afferents [1–4]. Naito *et al*. [4] showed that illusory elbow extension elicited by 80 Hz vibration on the skin over the left biceps tendon activated the right primary sensorimotor cortices (SM1) and a region located at the ventral part of the right supplementary motor area (SMA) and cingulate motor area (CMA). In this previous study, we could not fully exclude the possibility that these motor-related areas were partly activated by an 80 Hz vibration applied to the skin, since the control conditions involved vibration of the skin at different frequencies (10 Hz and 220 or 240 Hz). Thus, the aim of the present investigation was to test the hypothesis that SM1 and SMA/CMA are more active during kinesthetic illusions than when the skin surface beside the tendon is vibrated at the same frequency, but in a way that does not elicit any illusion.

In our previous study, we vibrated the tendons of left biceps muscles. In the present study we therefore vibrated the tendon of the right wrist extensor muscles to determine whether kinesthetic illusion would consistently activate the contralateral motor-related areas.

It remains unclear whether the sections of the motor-related areas that are activated by illusory movement of a body part are active during movement execution of the same body part. Therefore, we compared the activation pattern observed when subjects perceived the kinesthetic illusion of wrist movement with the activation pattern obtained in a previous study when subjects performed real wrist movement [5]. We expected that the illusion would activate the same parts of the SM1 and SMA/CMA that are activated during movement execution because the illusion is elicited mainly by afferent inputs from muscle spindles [6–8], which are also recruited during actual movement.

MATERIALS AND METHODS

Subjects and experimental conditions: Five right-handed healthy subjects participated in the PET experiment (ages 23–29 years). The study was approved by the Ethics Committee of the Karolinska Hospital and the Radiation Safety Committee of the Karolinska Institute and Hospital, and carried out following the principles and guidelines of the Declaration of Helsinki, 1975.

The subjects were blindfolded and positioned comfortably in a supine position on the bed of the PET scanner with their ears plugged. The right forearm of the subjects was supported proximal to the wrist and the wrist hung freely as demonstrated in Fig. 1. The wrist was completely relaxed in this position with the hand flexed at $42.0 \pm 2.4°$ (mean ± s.d.) at the wrist joint. The subjects were instructed to relax completely, refrain from moving, and to concentrate on the feeling in their right wrist. The experiment consisted of three conditions. In the rest condition (REST) the vibrator was held in the air close to the right wrist (~5 cm), but did not touch the skin. This ensured that the humming sound from the vibrator was matched in the comparisons with the other conditions. In the skin vibration condition (VIBRATION) we vibrated the skin surface

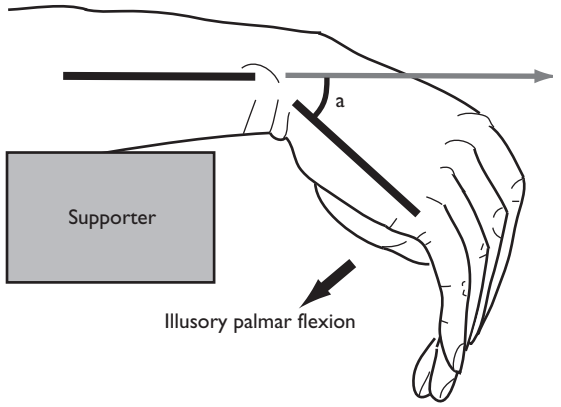

Fig. 1. The position of the right wrist. The wrist was completely relaxed throughout the experiment and hung freely. We measured the wrist angles from the original position (represented by a) with the aid of two small bars attached laterally to the surface of the skin over the wrist. After each ILLUSION condition, the subjects replicated the experienced maximum angles of the illusion by actually flexing their right wrist, and thus we could measure the angle of the illusory wrist flexion.

over the processes styloideus ulnae at 83 Hz by placing the vibrator in contact with the skin. This stimulus did not elicit an illusory wrist movement. In the tendon vibration condition (ILLUSION), we vibrated the surface of the skin over the tendon of the right extensor carpi ulnaris at 83 Hz. This stimulus elicits a vivid illusion of wrist palmar flexion.

After each condition the subjects were asked to describe what they had felt, and they were explicitly asked whether they had sensed an illusory wrist movement. If so, we asked them to demonstrate the experienced maximum angle of illusion by moving their right wrist. We then measured the illusory displacement of the wrist as the angle from the original position (Fig. 1).

In all conditions we used a vibrator with a small plastic spherical cap of about 1 cm diameter (Sasuri-Vib EV258-A, Matsushita Electronics, Osaka, Japan). The contact surface on the skin was $\sim 1\,cm^2$ for both test conditions and was marked on the surface of the skin. The mean distance between this tendon site, and the processes styloideus ulnae was 3.7 ± 0.7 cm. An experienced experimenter applied the vibrator at these sites with a constant pressure. During the experiments we monitored the muscle activity from the wrist flexor (the flexor carpi ulnaris) and extensor (the extensor carpi ulnaris) muscles of the right arm with surface electromyograms (EMGs).

PET scanning, image processing and statistical analysis: The relative rCBF was measured with a PET camera (ECAT Exact HR Siemens) operating in 3D mode. Twelve scans were collected for each subject. For each scan, about 13 mCi [^{15}O]butanol was injected i.v. as a bolus with each of the three conditions being repeated four times (the order of the conditions following a balanced pseudo-randomized schedule). Images of the radioactive counts per voxel (corresponding to rCBF) were generated by summing the activity during the 50 s immediately following the first increase in cerebral activity after the i.v. injection. The PET scans were reconstructed with a 4 mm Hanning filter and filtered with a 5 mm 3D isotropic Gaussian filter. For each subject we also acquired a high resolution T1 weighted anatomical MRI (1.5 T, Signa Horizon Echospeed, General Electric Medical Systems).

For each subject, all PET scans were spatially aligned to the first scan and co-registered to the MR image. The MR and co-registered PET images were normalized to the coordinate system of Talairach and Tournoux [9] using the standard brain [10] by a fast, automated full-multigrid (FMG) method [11]. The PET images were reformatted to isometric voxels ($2 \times 2 \times 2\,mm^3$), voxels outside the brain were excluded from the analysis. The statistical analysis was done in two parts. First, we analyzed the activity in the whole brain. This allowed us to examine the general pattern of brain activity associated with the two tasks (ILLUSION and VIBRATION). Then, to increase the sensitivity of our analysis, we used volume of interest (VOI) analysis for the SMA/CMA.

Whole brain analysis: We fitted a general linear model (GLM) to the PET data for every voxel in the brain [12]. In this model the design matrix had tasks and subjects as regressors. We defined linear contrasts between the conditions in the GLM, and the results of these contrasts are *t*-images (statistical images). We used the cluster simulation method of Ledberg [12] to determine the extent threshold for significantly active clusters (omnibus $p < 0.05$). The probability of finding false positive clusters throughout the whole brain space was estimated by Monte Carlo simulations of 2000 noise images [12]. This gave us a cluster size of $688\,mm^3$ and a t threshold of 2.68 as corresponding to an omnibus $p \leqslant 0.05$. Local maxima, (determined as a single voxel having the highest t value among all its neighboring 26 voxels), were also identified. Monte Carlo simulations showed that a t-value of 5.6 corresponded to omnibus $p < 0.05$ at the voxel level.

Identification of the regions that are active during real wrist movements: We used PET data from an independent group of eight right-handed healthy subjects [5] to identify the regions in the primary sensorimotor cortices (SM1) and the SMA/CMA that are active during real wrist movements. In this study, blindfolded subjects made auditory-paced alternating continuous extension and flexion movements of the right wrist at 1 Hz. This task was contrasted with a rest condition when the subjects made no movements. The PET scanning protocol was the same as used in the present kinesthetic illusion experiment. We now re-analyzed these PET data using identical image processing steps (e.g. a 5 mm 3D-Gaussian spatial filter, and normalization using the FMG method) and statistical analysis as used for the present experiment. At a threshold of $t = 3.25$ at each voxel, a cluster size of $400\,mm^3$ was significant [12]. We used this significance criterion since it gave us one cluster covering the left SM1 and one cluster located in the SMA/CMA (used to define the VOI, see later). Finally, we describe the overlap between the active clusters associated with the kinesthetic illusions and the active clusters related to movement execution (in a purely descriptive approach).

Anatomical definitions: We used cytoarchitecturally de-

fined areas from 10 post-mortem brains to indicate the probable locations of cytoarchitectonic areas 4a, 4p, 3a, 3b and 1 in the standard anatomical space [13,14]. The brains were corrected for deformations attributable to histological processing and the images were warped to the same standard anatomical format as the PET images using the FMG method [11]. The cytoarchitectural area assigned to each voxel in standard anatomical space was that with the largest number of post-mortem brains associated with it [15,16]. To allocate a voxel to an area rather than to parts of the cortices for which we have no available microstructural data (e.g. anterior to area 4a), the voxel had to be located in the microstructurally defined brain area in at least three of the 10 post-mortem brains. The result of this procedure is a probability map that provides a working definition of the probable location of each area in the standard anatomical space. The significant clusters were superimposed on the map and overlapping volumes were measured in mm^3 within each cytoarchitectonic area. The results are summarized in Table 1. For each site of the local maxima, we describe how many post-mortem brains (as a percentage of the 10 brains) have cytoarchitectonic areas 4a, 4p, 3a, 3b and 1 represented at these locations. We summarized the result for each cytoarchitectonic area in Table 2.

We used the definitions of the functional areas (dorsal premotor cortex (PMD), SMA and CMA) in the cortical motor system as defined by Roland and Zilles [17].

Volume of interest (VOI) analysis: For the SMA/CMA, the VOI was defined as the cluster (obtained from the independent group of subjects executing the wrist movements) located in the left hemisphere on the medial to the sagittal plane at $x = +10$. We normalized the mean global PET data from all subjects and scans as 50. This gave us a coefficient for normalization of each scan. Then, we normalized the mean PET data in the VOI by multiplying by the corresponding coefficient scan by scan. We did the same procedure in all three conditions. The analysis was made using GLM as implemented in the statistical software package SPSS (Version 10.0J, SPSS Japan Inc., Tokyo Japan). Tasks, subjects and the interaction between them were included as factors. Since the effect of task was significant in the VOI, we used a *t*-test to compare tasks (with a Bonferroni correction for multiple comparisons).

Table 1. Significant active fields in ILLUSION, VIBRATION and real wrist movements.

Structures	Coordinates of local maxima			*t*-value	Cluster (mm^3)	Overlap (mm^3)
	x	y	z			
Illusion *vs* Rest					6830	
Left M1	36	−18	52	5.2		
area 4a*	(30	−30	57)			922
area 4p*	(29	−34	49)			198
Left PMD	30	−22	58	4.9		
Left SI	30	−37	52	6.8		
area 3b*	(32	−35	51)			543
area 1*	(29	−40	59)			1484
Vibration *vs* rest					2716	
Left SI	48	−34	41	4.3		
area 1*	(49	−33	43)			144
Left supramarginal	50	−30	32	3.7		
Left PO	50	−28	23	4.0		
Left insula	44	−32	14	4.6		
Illusion *vs* vibration					1209	
Left M1	32	−33	52	6.0		
area 4a*	(31	−32	54)			321
area 4p*	(31	−33	49)			105
Left SI	28	−40	57	3.6		
area 3b*	(31	−35	51)			297
area 1*	(29	−39	57)			234
Real movement *vs* rest					30544	
Left M1	28	−31	58	15.0		
area 4a*	(29	−28	56)			3727
area 4p*	(28	−29	47)			2031
Left PMD	30	−16	54	4.7		
Left SI	38	−28	48	12.4		
area 3a*	(29	−31	41)			1055
area 3b*	(35	−31	49)			1894
area 1*	(37	−35	56)			4498
Left SMA CMA	6	−16	44	9.5		
Left PO	46	−26	21	5.2		
Left insula	38	−32	17	5.2		

M1, primary motor cortex; PMD, dorsal premotor cortex; SI, primary somatosensory cortex; SMA, supplementary motor area; CMA, cingulate motor area; PO, parietal operculum.
Coordinates in Talairach and Tournoux [9] (ECHBD: Roland *et al.* [10]).
*Note that the coordinates for the cytoarchitectonic areas are the center of gravities.
*Descriptive overlapping volumes with each cytoarchitectonic area were measured.

Table 2. Location of local maxima in the cluster of ILLUSION *vs* VIBRATION and their probable cytoarchitectonic areas.

Coordinates			*t* value	Cytoarchitectonic areas				
x	y	z		area 4a	area 4p	area 3a	area 3b	area 1
32	−33	52	6.02	30%	0	0	10%	0
40	−36	48	3.28	0	0	0	0	20%
28	−40	58	3.61	0	0	0	10%	50%

% indicates how large a percentage of the 10 post-mortem brains was represented in each cytoarchitectonic area. A voxel (32, −33, 52) was also significantly activated from whole brain simulations.

RESULTS

All subjects reported that they experienced a vivid illusory sensation of a palmar flexion of the right wrist in the ILLUSION, but not in VIBRATION or REST conditions. Their wrists did not move in any of the three conditions. Surface EMG did not detect any activity from the flexor (agonistic) muscle of the wrist. The mean illusory angle of palmar flexion was $18.7 \pm 5.0°$ from the original relaxed position.

In the whole brain analysis, a cluster covering the contralateral (left) primary sensorimotor cortices (SM1; cytoarchitectonic areas 4a, 4p, 3b and 1) extending anteriorly into the dorsal premotor cortex (PMD) was significantly activated when we used the contrast of ILLUSION *vs* REST (Table 1). In addition, a trend for increases in activation was observed in the contralateral SMA/CMA (at the threshold of a cluster size of 624 mm^3, omnibus $p = 0.0825$). The VIBRATION condition did not activate the precentral gyrus, SMA or CMA, but did activate the left primary somatosensory cortex (SI; cytoarchitectonic area 1), supramarginal gyrus, parietal operculum (PO) and insular cortex when compared with rest (Table 1, Fig. 2a).

When ILLUSION was contrasted with VIBRATION, differentiating the effect of illusion from that of vibration, a cluster covering the contralateral SM1 (cytoarchitectonic areas 4a, 4p, 3b and 1) was significantly activated (Table 1, Fig. 2b). The local maxima of the activation were located in the population map of cytoarchitectonic areas 4a and 1 (Table 2).

When real movement was contrasted with rest in order to identify the regions in the SM1, SMA and CMA that are active during real movements of the right wrist, a cluster covering the left SM1 (cytoarchitectonic areas 4a, 4p, 3a, 3b and 1), SMA, CMA, PMD, PO and insular cortex was significantly activated (Table 1). The cluster associated with the illusory movement (ILLUSION *vs* VIBRATION) corresponded to a sub-volume of SM1 section activated during the real movements (Figure 2b).

In the VOI analysis, we found that the SMA/CMA region activated during the real movement (Fig. 2c) was more active in the ILLUSION condition than in the VIBRATION condition ($p < 0.05$ after Bonferroni correction for multiple comparisons; Fig. 2d).

DISCUSSION

The present results suggest that kinesthetic illusion of a right wrist movement activates the contralateral primary sensorimotor cortices (SM1; cytoarchitectonic areas 4a, 4p, 3b and 1) and a field located in the SMA and CMA in the absence of real movement. The increases in activity in these areas probably reflect the kinesthetic illusions because, in the control condition, the skin was vibrated at the identical frequency of 83 Hz without eliciting an illusion. This result, together with the results from our previous study [4], strongly suggests that kinesthetic illusions of limb movements activate motor-related areas. In addition, these active motor areas are contralateral to the illusory limb movements when vibrating the right wrist and left biceps

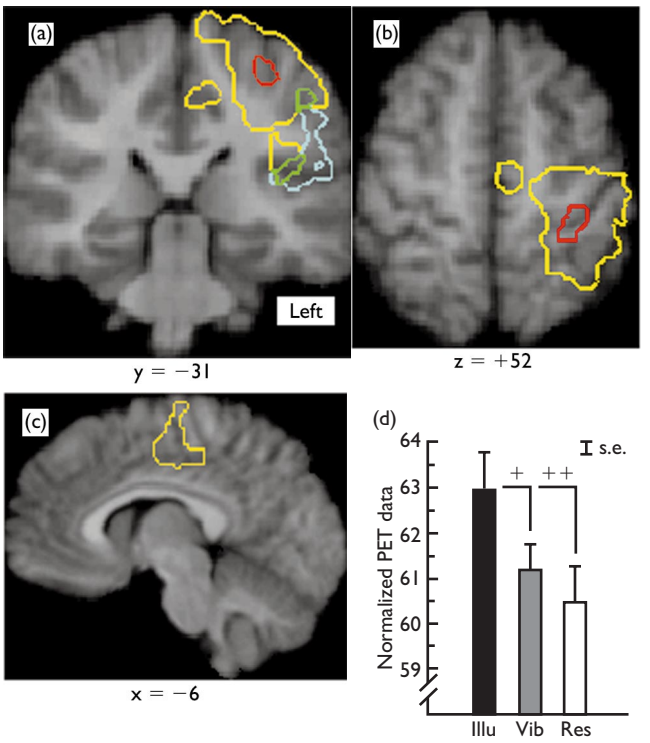

Fig. 2. Whole brain activation maps (omnibus $p < 0.05$) and result from volume of interest (VOI) analysis. Areas encircled with yellow lines represent the significant clusters in the contrast between real wrist movement *vs* rest. (**a**) Areas represented by green and light blue lines indicate activation in VIBRATION *vs* REST. Areas with green lines indicate overlapping sections between VIBRATION *vs* REST and real movement *vs* rest [5]. (**a**,**b**) Red lines indicates significant activation in ILLUSION *vs* VIBRATION. (**c**) The SMA/CMA cluster obtained from the real wrist movements which was used to define the VOI (See Materials and Methods). (**d**) Normalized PET data in the volume of interest (VOI). The normalized PET data in the three conditions (ILLUSION, VIBRATION and REST) from the SMA/CMA. We observed significantly greater activity in ILLUSION than in VIBRATION. $^{+}p < 0.05$; $^{++}p < 0.005$.

muscles [4]. Furthermore, our results indicate that the motor fields activated during kinesthetic illusions of limb movements are active during movement execution of the same limb.

In the two conditions, we vibrated two sites (< 4 cm apart) over the skin around the wrist at the same frequency. One may presume the same types of skin receptors are recruited during the vibration. We think that it is unlikely that the afferent inputs from the skin receptors on the different sites of wrist could produce the conspicuous differences in activation patterns seen in the two conditions (Fig. 2a). Thus, the activation associated with the illusion reflect afferent inputs from vibrated tendon. The activation we found in the SM1 associated with the kinesthetic illusion probably engaged the primary motor cortex (M1), at least in part. Our reasoning behind this is that (i) the active cluster engaged the precentral gyrus in all subjects (as determined from the normalized MR images of individual subjects), and (ii) the local maxima of the activation was located in the population map of cytoarchitectonic area 4a (see Materials and Methods and Table 2). One should bear in mind, however, that the restricted spatial resolution of activation maps (PET data from a group of subjects) means that we can not exclude the possibility that some of the activity we observed in the cytoarchitectonic map of each area might to some extent reflect activity from the adjacent cytoarchitectural fields.

Our main result shows that motor-related areas are involved in processing of inputs from muscle spidles and probably central processing of human kinesthesia. The activation of contralateral M1 fits well with the notion that this area is one of the cortical targets for muscle spindle afferents as shown in monkeys [18]. Indeed, the physiological mechanism underlying the illusory experience is the central processing of the afferent inputs from muscle spindles [6–8]. Furthermore, in the monkey brain, neurons in SMA and CMA are activated by passive movements of the limbs [19,20]. Passive movements activate human SMA [21]. Furthermore, electrical stimulation at certain sites in human SMA and CMA can elicit movement sensation without generating actual movements [22,23].

A second observation was that the kinesthetic illusion activated fields of the SM1 and the SMA/CMA that are active when subjects executed wrist movements. We are aware that when we compare the PET images from one group of subjects performing real movements with another group of subjects experiencing the illusion, we can only conclude that similar regions were activated, but we cannot determine whether exactly the same small groups of neurons (or single voxels, as this is the limit of our resolution) were activated. However, the SM1 section activated during the wrist illusion is most probably the wrist section of SM1 because real wrist movements performed by the independent group of subjects also activated the very same part of this area. This suggests that the section active in the SM1 during kinesthetic illusion of a given limb might be somatotopically organized. Indeed, it is known that identical neurons, which are associated with the generation of movements, in the primary motor cortex, SMA and CMA in monkeys are also recruited by passive movements of the identical limb [18–20,24,25]. Thus, the present results, together with these earlier single cell recordings, suggest that kinesthetic illusions and movement execution engage some common neural populations in the motor cortices.

CONCLUSION

Kinesthetic illusion of a right wrist movement activates the contralateral primary sensorimotor cortices (SM1; cytoarchitectonic areas 4a, 4p, 3b and 1) and a field located in the SMA and CMA in the absence of real movement. This finding corroborates the results from our previous study [4] and strongly suggests that kinesthetic illusion of limb movement activate the contralateral motor-related areas. Furthermore, our results indicate that the motor fields activated during kinesthetic illusion of a limb movement are active during movement execution of the same limb.

REFERENCES

1. Goodwin GM, McCloskey DI and Matthews PBC. *Brain* **95**, 705–748 (1972).
2. Goodwin GM, McCloskey DI and Matthews PBC. *Science* **175**, 1382–1384 (1972).
3. Craske B. *Science* **196**, 71–73 (1977).
4. Naito E, Ehrsson HH, Geyer S *et al*. *J Neurosci* **19**, 6134–6144 (1999).
5. Ehrsson HH, Naito E, Geyer S *et al*. *Eur J Neurosci* **12**, 3385–3398 (2000).
6. Burke D, Hagbarth K, Lofstedt L *et al*. *J Physiol (Lond)* **261**, 673–693 (1976).
7. Roll JP and Vedel JP. *Exp Brain Res* **47**, 177–190 (1982).
8. Roll JP, Vedel JP and Ribot E. *Exp Brain Res* **76**, 213–222 (1989).
9. Talairach J and Tournoux P. *A Co-Planar Stereotaxic Atlas of the Human Brain*. New York: Thieme; 1988.
10. Roland PE, Svensson P, Fredriksson J *et al*. *Soc Neurosci Abstr* **24**, 2094 (1998).
11. Schormann T and Zilles K. *Hum Brain Mapp* **6**, 339–347 (1998).
12. Ledberg A. *Hum Brain Mapp* **9**, 143–155 (2000).
13. Geyer S, Ledberg A, Schleicher A *et al*. *Nature* **382**, 805–807 (1996).
14. Schleicher A, Amunts K, Geyer S *et al*. *Neuroimage* **9**, 165–177 (1999).
15. Roland PE and Zilles K. *Neuroimage* **4**, 39–47 (1996).
16. Roland PE and Zilles K. *Brain Res Rev* **26**, 87–105 (1998).
17. Roland PE and Zilles K. *Curr Opin Neurobiol* **6**, 773–781 (1996).
18. Colebatch JG, Sayer RJ, Porter R *et al*. *Electroencepharogr Clin Neurophysiol* **75**, (1990).
19. Hummelsheim H, Bianchetti M, Wiesendanger M *et al*. *Exp Brain Res* **69**, 289–298 (1988).
20. Cadoret G and Smith AM. *J Neurophysiol* **73**, 2584–2590 (1995).
21. Weiller C, Juptner M, Fellows S *et al*. *Neuroimage* **4**, 105–110 (1996).
22. Fried I, Katz A, McCarthy G *et al*. *J Neurosci* **11**, 3656–3666 (1991).
23. Lim SH, Dinner DS, Pillay PK *et al*. *Electroencepharogr Clin Neurophysiol* **91**, 179–193 (1994).
24. Lemon RN, Hanby JA and Porter R. *Proc R Soc Lond B Biol Sci* **194**, 341–373 (1976).
25. Fetz EE, Finocchio DV, Baker MA *et al*. *J Neurophysiol* **43**, 1070–1089 (1980).

Acknowledgements: This study was supported by the Volvo Foundation. E.N. was supported by the Naito Foundation in 1998 and by a the research grant for foreign research for young scientists from the ministry of education of Japan in 2001. H.H.E. was supported by the Axel and Margaret Axson Johnsson's foundation and Stiftelsen Sunnerdahl. We thank Professor P.E. Roland for valuable scientific comments and Dr B. Gulyas for technical assistance. We also appreciate the work of the late Mr Walter Pulka on the tracer synthesis.